Full Paper
doi.org/10.1002/chem.202003448

Polycycles |Hot Paper|

Carbon Origami via an Alumina-Assisted Cyclodehydrofluorination Strategy

Ann-Kristin Steiner,[a] Dmitry I. Sharapa,[b] Sergey I. Troyanov,[c] Jürgen Nuss,[d] and Konstantin Amsharov*[a, e, f]

Abstract: The synthesis of pristine non-planar nanographenes (NGs) via a cyclodehydrofluorination strategy is reported and the creation of highly strained systems via alumina-assisted C–F bond activation is shown. Steric hindrance could execute an alternative coupling program leading to rare octagon formation offering access to elusive non-classical NGs. The combination of two alternative ways of folding could lead to the formation of various 3D NG objects, resembling the Japanese art of origami. The power of the presented "origami" approach is proved by the assembly of 12 challenging nanographenes that are π-isoelectronic to planar hexabenzocoronene but forced out of planarity.

Introduction

The chemistry of large polycyclic aromatic hydrocarbons (PAHs) is nowadays flourishing more than ever in the form of atomically precise nanographenes (NGs).[1] The exploding interest originates from the virtually unlimited number of variations in size and shape which dictate the unique electronic and optical properties of NGs.[2–4] However, the properties of NGs can be also effectively tuned by the converting inherently 2D-NGs into 3D objects. Metaphorically, any 3D-NGs can be imagined as a fragment of a graphene sheet cut with imaginary scissors and folded up like an origami figure. Instead of scissors, the bottom-up approach provides a piece of "carbon-paper" of required size, while non-hexagonal rings or helical motive allow 3D-molecular folding. Rational incorporation of these elements would penetrate the barrier between macro- and micro-worlds for the engineering of carbon-based materials with functional molecular shapes. Considering the possible complexity of macroscopically folded pieces of paper, artificial molecular folding of NGs is nowhere near as advanced as the handmade technique. Here, we demonstrate that alumina-mediated C–F bond activation appears to be a superior strategy to tackle this challenge since it allows both the effective incorporation of non-hexagonal rings and the formation of helical structures. Based on the example of 12 isoelectronic NGs, we show that the HOMO–LUMO gap can be tuned in a wide range depending on the type of folding.

In general, the geometry of NGs can be forced into non-planarity either by embedding non-hexagonal rings into the graphene framework,[5–13] or by steric strain originating from atom crowding.[14–16] However, as a result of high strain the synthetic access to this class of compounds remains rather scarce. The Scholl reaction, which was proven to be a powerful method for the synthesis of planar NGs,[17] typically reaches its limits in the case of strained non-planar systems. As a result of the cationic nature,[18,19] the Scholl reaction tends to give rise to skeletal rearrangements frequently yielding undesired products.[20–22]

Recent progress in the intramolecular aryl-aryl coupling via C–F bond activation reveals a high potential of the approach for the controllable synthesis of complex NGs.[23–27] In particular, it has been demonstrated that cyclodehydrofluorination (CDHF) on alumina is a powerful alternative which can address many of the above-mentioned limitations.[28–31] Thus, it was possible to incorporate pentagons into various PAHs, nearly

[a] A.-K. Steiner, Prof. Dr. K. Amsharov
Department of Chemistry and Pharmacy, Institute of Organic Chemistry
Friedrich-Alexander-University Erlangen-Nuremberg
Nikolaus-Fiebiger-Straße 10, 91058 Erlangen (Germany)
E-mail: konstantin.amsharov@fau.de

[b] Dr. D. I. Sharapa
Institute of Catalysis Research and Technology
Karlsruhe Institute of Technology (KIT), Herrmann-von-Helmholtz-Platz 1
76344 Eggenstein-Leopoldshafen (Germany)

[c] Prof. S. I. Troyanov
Department of Chemistry, Lomonosov Moscow State University
Leninskie gory, 119991 Moscow (Russia)

[d] Dr. J. Nuss
Max Planck Institute for Solid State Research
Heisenbergstraße 1, 70569 Stuttgart (Germany)

[e] Prof. Dr. K. Amsharov
South Ural State University, pr. Lenina 76, 454080 Chelyabinsk (Russia)

[f] Prof. Dr. K. Amsharov
Institute of Chemistry, Organic Chemistry
Martin-Luther-University Halle-Wittenberg
Kurt-Mothes-Strasse 2, 06120 Halle (Germany)

Supporting information and the ORCID identification number(s) for the author(s) of this article can be found under: https://doi.org/10.1002/chem.202003448.

quantitatively producing strained bowl-shaped systems which are not accessible by cyclodehydrogenation.[28–31]

Further, it has been shown that C–F bond activation allows controllable cyclization in a domino-like manner.[32,33] This provides essential flexibility in the precursor design and control over the formation of the desired C–C bonds.[34]

In this work we explored the applicability of the HF-zipping approach for the synthesis of multihelical NGs which are difficult to obtain by existing methods. The well-known planar hexa-*peri*-hexabenzocoronene (HBC) was chosen as a model NG pattern. In order to demonstrate the power of HF zipping, we performed partial condensation of the selected bonds in HBC and generated three challenging structures (**N1**,**N11** and **N15**) which are isoelectronic to HBC. We show that such a transformation is not only feasible but also presents a general route to the non-planar NGs. It is noteworthy that all target compounds are not accessible via Scholl oxidation and require individual synthetic approaches using harsh conditions or highly reactive aryne intermediates (Figure 1). Furthermore, it was found that the steric hindrance could cause an alternative HF-zipping program, leading to effective eight-membered ring formation (Figure 1). The algorithm of cyclizations appears to be predictable from the structure and thus can be controlled by the proper design of the precursor. This finding opens a general access not only to various twisted multihelical NGs but also to rare grossly warped NGs containing cyclooctatetraene fragments.[41,42]

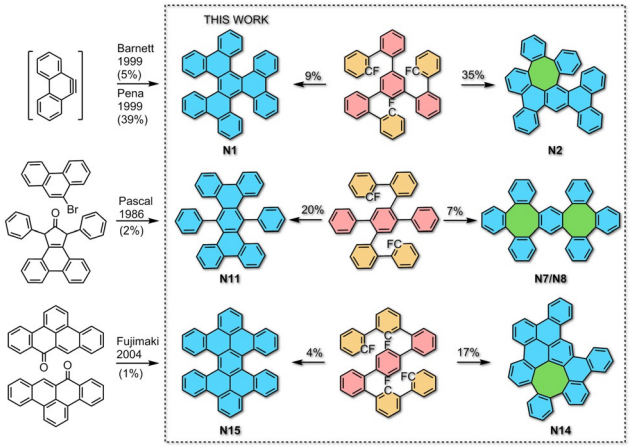

Figure 1. Selected non-planar NG structures π-isoelectronic to HBC obtained in this work: hexabenzo[*a*,*cd*,*f*,*j*,*lm*,*o*]perylene (**N15**),[35] 9,18-diphenyltetrabenzo[*a*,*c*,*h*,*j*]anthracene (**N11**),[36–37] and hexabenzo[*a*,*c*,*g*,*i*,*m*,*o*]tri-phenylene (**N1**).[38–40] On the right the unexpectedly effective alternative folding leading to the rare octagon containing NGs (**N2**, **N7**/**N8** and **N14**) is presented.

Results and Discussion

The strong C-F bond tolerates the majority of reactions providing essential flexibility in the synthesis of fluoroarene precursors and rather simple access to the target NGs. Thus, relatively complex precursor molecules **P1**–**P4** used in this study were obtained by exploiting a one-step Suzuki coupling of the fluorinated arylboronic acids with arylbromides, as is shown in Figure 2. (For details see Supporting Information). The respective CDHF reactions were carried out in the presence of activated γ-aluminum oxide using microwave heating and the reaction outcome was monitored by HPLC/UV/MS analysis.[30] Precursor **P1** preprogrammed for the triple HF elimination was expected to condense to hexabenzotriphenylene **N1** as shown in Figure 1. Condensation of **P1** at 210 °C for 18 h reveals the completion of HF zipping leading exclusively to the product of a three-fold HF elimination (isolated yield 75 %). Surprisingly, along with the formation of target **N1** (9 %) the major components of the reaction were found to be **N2** (35 %,) and **N3** (31 %) which also represent products of three-fold HF elimination (Figure 3). The NMR spectra of **N2** and **N3** revealed the low symmetry of both products and showed characteristic signals below 7.0 ppm, which are typical for protons placed above the aromatic ring plane denoting the non-planar geometry. Additionally, six and seven bay-region protons (8.2–8.8 ppm) can be assigned for products **N2** and **N3**, respectively. Detailed NMR analysis supported by DFT calculations allowed assignment of **N2** and **N3** to NGs containing an eight-membered ring as displayed in Figure 3.

Finally, the connectivities of both compounds were unambiguously determined by single-crystal X-ray analysis. Additionally, the reaction was performed at a lower temperature (200 °C for 5 h) allowing isolation and characterization of all key intermediates (for details see Supporting Information). Detailed analysis of the intermediates and products showed that on the second and third cyclization steps the formation of the eight-membered ring appears to be preferable. It is noteworthy that the cyclization is characterized by a clean conversion

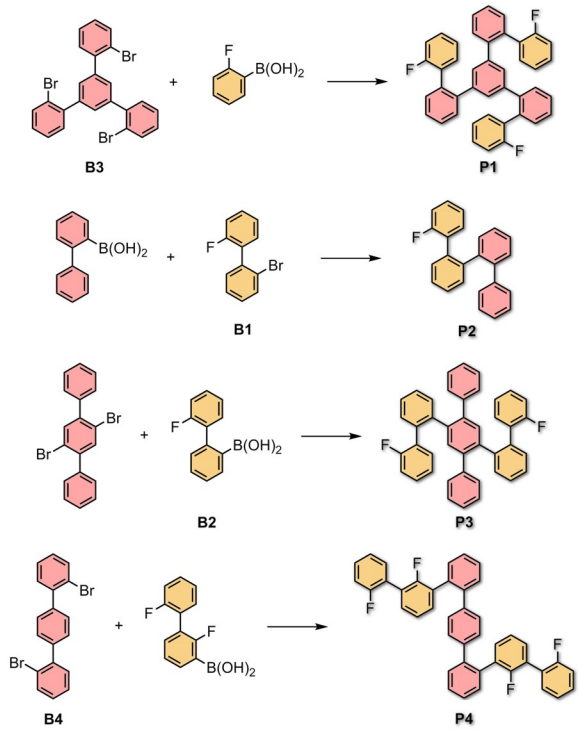

Figure 2. Synthesis of precursor structures **P1**–**P4**: Pd(dppf)Cl_2, K_3PO_4, toluene/H_2O, reflux; **P1**: 68 %; **P2**: 63 %; **P3**: 95 %; **P4**: 88 %.

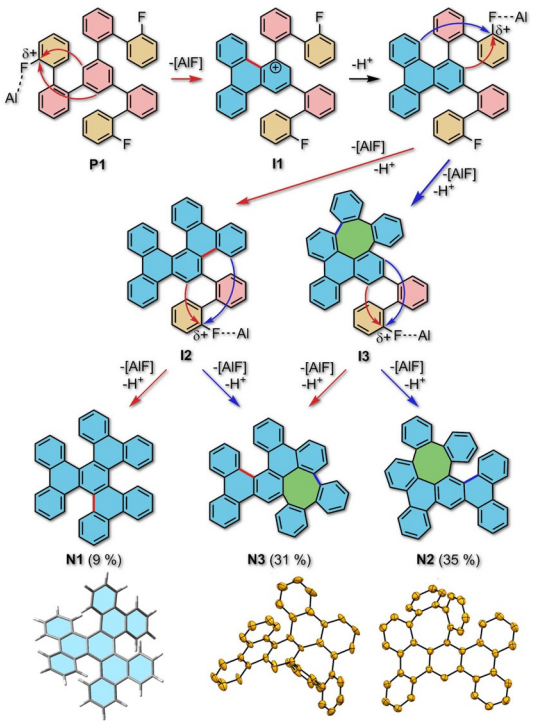

Figure 3. Proposed mechanism of **P1** cyclization to **N1**, **N2** and **N3** showing the formation of the expected intermediate **I1** at the first step and switching the regioselectivity at the second step resulting in the preferable formation of **I3** containing an eight-membered ring (blue arrow), instead of the formation of helical **I2** (red arrow). DFT-optimized structure of **N1** and single crystal X-ray structures of **N2** and **N3** depicted as ORTEP projections are shown at the bottom.

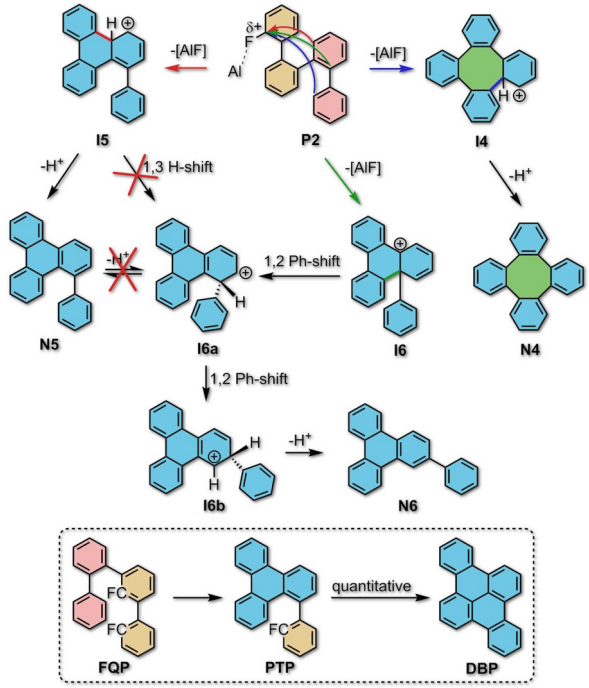

Figure 4. Supposed mechanism showing the three competitive pathways of **P2** cyclization: eight-membered ring formation (blue arrow) leading to tetraphenylene (**N4**); six-membered ring formation (red arrow) leading to **N5**; *ipso*-attack (green arrow) leading to **I6** which undergoes rearrangement via migration of the phenyl residue resulting in **N6**. Bottom: synthesis of dibenzopyrene (**DBP**) from fluorinated quaterphenyl (**FQP**) in nearly quantitative yield demonstrating stability of the **TPT** intermediate to the rearrangement under CDHF reaction conditions.[32]

to the strained **N1**, **N2** and **N3** without any sign of rearrangements and formation of other side products. A possible mechanism of **P1** condensation is depicted in Figure 3. According to our DFT study the CDHF reaction can be described as a synchronous Friedel–Crafts-like arylation process.[33] Namely, the polarization of the C–F bond leads to the formation of an electrophilic center (C–F carbon) which can be attacked by the neighboring electron-rich π-system. During the first cyclization both possible attacks provide the same triphenylene core (**I1**). Since the second HF elimination to **I2** requires the formation of a strained [5]-helicene substructure the regioselectivity is switched toward the eight-membered ring formation yielding **I3** as a major product. The resulting **I3** has only two alternative folding ways leading to final **N2** and **N3** (Figure 3).

To support the proposed mechanism, we have analyzed the single HF-elimination on model fluorinated quaterphenyl **P2** containing an additional phenyl substituent which should appear in the sterically hampered bay region of the triphenylene core after cyclization (Figure 4, structure **N5**). Since the formation of **N5** is accompanied by the steric hindrance the formation of an eight-membered ring yielding tetraphenylene **N4** could be expected. The reaction outcome was monitored by HPLC, which revealed a clean conversion to three compounds: **N4** (3 %),[43] target **N5** (44 %), and **N6** (38 %). The formation of **N6**, accompanied by the migration of the phenyl group was investigated additionally. As depicted in Figure 4 there are at least two competing pathways of the ring formation in **P2** leading to either protonated tetraphenylene **I4** (blue arrow) or protonated phenyltriphenylene **I5** (red arrow). In general, the cationic nature of both intermediates could give rise to 1,2-phenyl migration, thus yielding the **N6**. However, none of the directly formed intermediates (**I4**, **I5**) appears to be suitable for the rearrangement. A fairly unlikely scenario would require formal 1,3-migration (two successive 1,2-migrations) of the proton in **I5** yielding **I6a** which is able to undergo a 1,2-phenyl shift leading to **I6b**. However, this mechanism is not consistent with the cyclization of the model of fluorinated quaterphenyl (**FQP**) yielding dibenzopyrene (**DBP**) with close to quantitative yield without any sign of the rearrangement of intermediate phenyltriphenylene (**PTP**) (Figure 4).[32] The second probable scenario includes protonation of the final **N5** leading to **I6a** which is expected to undergo 1,2-phenyl shift before rearomatization yielding a thermodynamically more stable isomer **N6**.This possibility was ruled out by the test experiment demonstrating that **N5** remains intact under CDHF reaction conditions. This leads to the assumption that the rearrangement could only be implemented via *ipso*-attack. As is shown in Figure 3 (green arrow) the *ipso*-attack leads to triphenylene cation **I6** which can directly undergo two subsequent 1,2-phenyl shifts leading to the cationic intermediate **I6b** whose final deprotonation results in **N6**. Note that the nearly quantitative formation of model **DBP** from **FQP** is connected with

the **FQP** structure where both the eight-membered ring formation and the *ipso*-attack are impossible.

These results show that if the inherently favorable hexagon formation is sterically hampered then the regioselectivity can be switched towards either non-hexagonal ring formation or spiro-intermediates. The observed rearrangement appears to be a direct consequence of the alternative CDHF algorithm and thus can be rationally suppressed or directed.

These observations, especially the fact of *ipso*-attack during CDHF reaction turned out to be very important in the case of precursor structure **P3** since it contains two flexible phenyl substituents providing a suitable geometry for *ipso*-attack. Not surprisingly, the cyclization of **P3** displays the formation of seven isomeric compounds (see Supporting Information, Figure 5 and Figure 6). All products were isolated by preparative HPLC and characterized by means of NMR, MS and X-ray analysis. All isolated NGs show the same *m/z* ratio of 530 indicating that all compounds are the products of successful twofold HF elimination. Detailed analysis of proton NMR supported by DFT calculation allows to assign the structures of all isomers (see Supporting Information). Considering the effective eight-membered ring formation discussed above, one of the cyclization scenarios in **P3** leads to the tribenzo[3,4:5,6:7,8]cyclooctа[1,2-*b*]tetraphenylene (**N7**/**N8**) representing a highly interesting class of compounds with negative Gaussian curvature. The mechanism for the formation of both structures is depicted in Figure 5. Indeed, both *cis*- (**N7**) and *trans*- (**N8**) isomers were found in the reaction mixture and isolated in 3% and 4% yield, respectively. It is noteworthy that **N7**/**N8** conformers do not interconvert into each other and can be separated in pure form allowing to elucidate the structure by means of NMR spectroscopy. Finally, single crystals X-ray analysis unambiguously confirmed the generation of **N7** and **N8**.

In absolute agreement with our expectations, the next compound was identified as **N9** (16% yield) which forms after six- and eight-membered ring formation regardless of the order of cyclizations, as is shown in Figure 5. The connectivity of **N9**

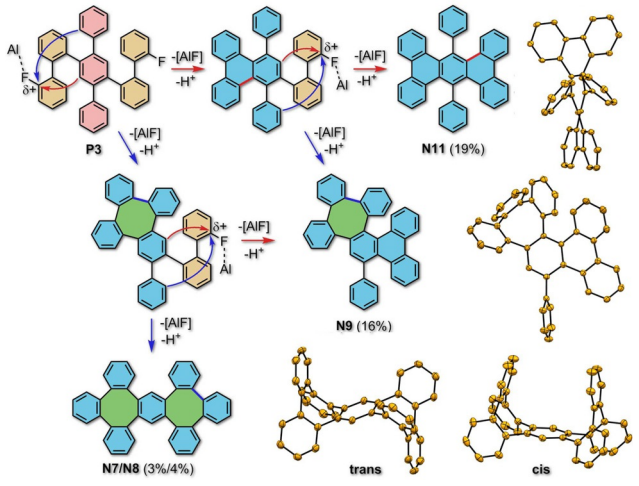

Figure 5. Alternative condensation pathways of **P3** leading to **N7**, **N8**, **N9** and **N11** and respective single crystal X-ray structures depicted as ORTEP projection at the 30% probability level.

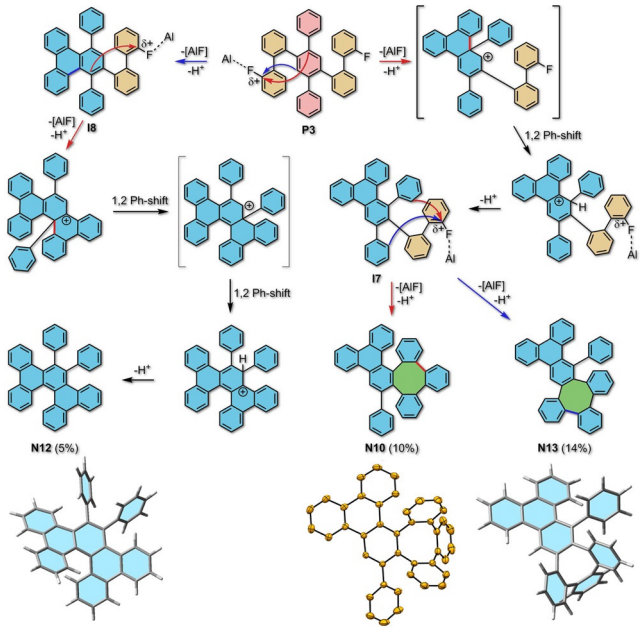

Figure 6. Alternative pathways of **P3** condensation leading to **N10**, **N12** and **N13** showing effective *ipso*-attacks during cyclization. Bottom: DFT optimized structures of **N12** and **N13**, and ORTEP plot of **N10** (displacement ellipsoids are drawn at the 30% probability level).

was unambiguously proven by the crystallographic analysis. Finally, known target nanostructure **N11** was isolated with 19% yield. The ^{1}H-NMR spectrum of **N11** was found to be in agreement with the literature data.[37,44] The next two products were assigned to nanostructures **N10** (10%) and **N13** (14%). The connectivity of **N10** was confirmed by single crystal X-ray analysis. A possible pathway for **N10** and **N13** formation, depicted in Figure 6, includes an *ipso*-attack on the first reaction step which is in line with our observations that were drawn for the cyclization of **P2**.

The last compound identified in the reaction mixture displays high symmetry according to NMR analysis and contains two triphenylene fragments and no eight-membered rings in the structure. Detailed analysis of NMR data allows us to assign it to the helicene **N12** (5%) and finally to confirm our assignment by the comparison of NMR spectra with the previously reported data.[45,46] As displayed in Figure 6 the most probable pathway of **N12** formation includes one hexagon formation and one *ipso*-attack followed by two subsequent 1,2-phenyl shifts. Note that all seven compounds identified in the reaction mixture are theoretically expected when considering the possible cyclization pathways.

As noted in the above, the CDHF reaction can be effectively performed in a domino-like fashion, which notably extends the synthetic scope of the reaction.[32] In this regard, we additionally investigated whether the zipping approach can be applied for the synthesis of multihelical nanographenes. Precursor **P4** preprogrammed for fourfold HF elimination was selected as a representative model. The complete cyclization of **P4** was achieved at 200 °C for 15 h indicating the formation of several compounds and one major product (see Supporting Informa-

tion). The major product (17% isolated yield), however, was not identified as the desired hexabenzoperylene **N15** since the UV spectrum was not consistent with the previously published data.[11,42] Instead, one of the minor fractions (see Supporting Information) was assigned to **N15**. Both products were separated by preparative HPLC and analyzed by NMR and LDI MS. Although **N15** was isolated in only 4% yield the suggested synthetic route appears to be the best approach to pristine **N15** since the previously reported strategy provides **N15** in only a 1% yield.[35] The major product shows the same *m/z* ratio of 526 as the desired **N15** indicating successful fourfold HF-elimination. Detailed analysis of ^{1}H NMR spectrum supported by DFT calculation (see Supporting Information) allows us to assign a major product to nanographene **N14** containing an eight-membered ring as depicted in Figure 6. The assignment was confirmed by X-ray analysis of a single crystal of **N14**. To explain the relatively high selectivity in the formation of **N14** the pathway from **P4** to **N14** was investigated theoretically at the DFT level. Analysis of the possible pathways reveals that **N14** can be formed via formation of a spiro intermediate only. As depicted in Figure 7 the first two CDHF reactions occur, as discussed in the above, resulting in the formation of a dibenzopyrene segment (**I7**). Further cyclization could either lead directly to the cation **I8** or to the isomeric spiro intermediate **I9**. According to our DFT calculations it is not necessary to distinguish which attack proceeds faster since both isomers can easily interconvert into each other (see Supporting Information). Noteworthy that the spiro compound **I9** was found to be 12 kcal mol^{-1} more stable than **I8**. The resulting spiro intermediate **I9** cannot be stabilized by deprotonation before the rearrangement, which can be realized in two competing ways. Namely, it can either yield **I8** and the reaction will proceed further to **N15**, or yield helicene **I10**. Mechanistic consideration at the DFT level reveals that the transformation to **I10** appears to be more favorable from both a kinetic and a thermodynamic point of view (see Supporting Information). This explains the formation of **N14**, since **I11** has only one opportunity to undergo the last cyclization via eight-membered ring formation.

According to Clar's rule all twelve nanographenes obtained in this work formally belong to the class of all-benzoid compounds with seven Clar sextets. Therefore, the question of how the non-planar geometry influences the delocalization of electron density inside the molecule appears to be very interesting since all the presented systems can be compared. The NICS analysis reveals that the majority of molecules possess a pronounced all-benzoid character despite the geometrical perturbations (Figure 8).

Exceptions here are **N12** showing low aromaticity of the central ring and **N1** where the aromaticity of the central ring is completely "destroyed". Highly unexpectedly the central hexagons in **N15** and **N11** remain truly aromatic despite the even more pronounced deviation from the planar geometry. The bond length analysis is in line with NICS considerations, showing virtually equal bond lengths in **N15** (central hexagon) and notable bond length alternation in **N1** (central hexagon). Close inspection shows that the distortion of the hexagon leading to the chair-like geometry prevents the effective conjugation, whereas the distortion toward twisted (half-chair-like) geometry virtually does not affect the aromaticity (Figure 8). These results indicate that the way in which the benzene ring is "bent" plays more of an important role in terms of aromaticity than the actual degree of deviation from planarity. The introduction of an octagon into the system results in a saddle-shaped cyclooctatetraene geometry minimizing the conjugation, thus avoiding an antiaromatic character. This also explains why isomeric **N7** and **N8** are stable and do not interconvert into each other (the respective transition state is expected to possess pronounced an antiaromatic character). However, if the eight-membered ring is embedded into the rigid π-system the conjugation cannot be avoided. This results in the generation of a pronounced paratropic ring current inside the octagon reaching a value of 4.1 (**N14**) as indicated by the NICS(0) analysis. Despite the fact that all molecules have an isoelectronic π-

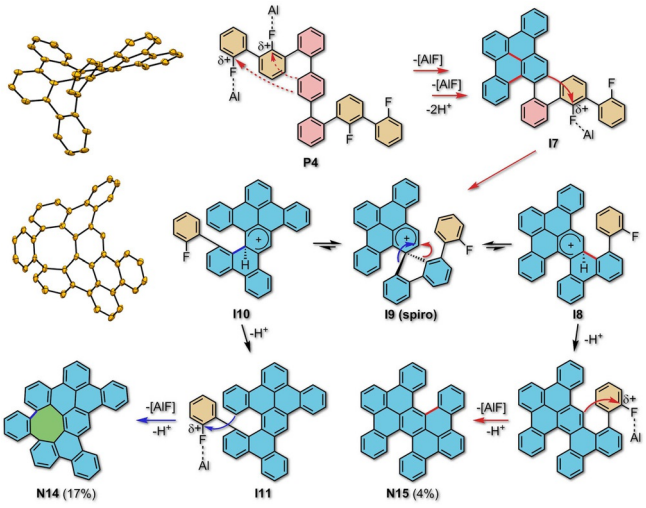

Figure 7. DFT predicted pathways from **P4** to **N14** and **N15** via a spiro intermediate **I9**. Middle left: ORTEP projection of **N14** (thermal ellipsoids are shown at the 30% probability level).

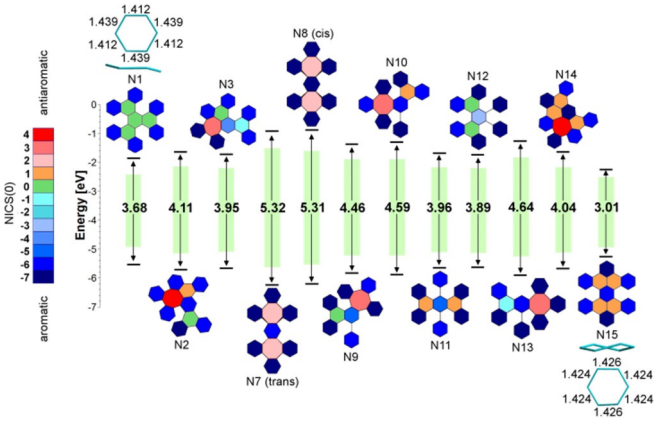

Figure 8. HOMO–LUMO gap and NICS(0) values of prepared NGs. Geometries of the central ring in **N1** (chair-like) and **N15** (half-chair-like) derived from DFT optimized structures. Geometric details of the central benzene rings of **N1** and **N15** are shown in inset. Bond lengths are given in Å. Experimentally obtained optical gaps are presented as green bars.

system the HOMO–LUMO gap can be varied in a wide range from 5.3 to 3.0 eV (Table 1), indicating the strong influence of the geometry on the electronic communication. The experimentally obtained optical gaps were found to be in accordance with the theoretically predicted optical gaps and show virtually linear correlation with the respective HOMO–LUMO gaps (see Supporting Information). It is noteworthy that the structure **N15** displays the lowest band gap of 3.0 eV which is rather close to the gap of tetracene. Such a low gap is highly counterintuitive and makes the compound **N15** highly interesting from a theoretical point of view, since the low band gap is typically connected with the high reactivity whereas the all-benzoic character is an indicator of enhanced stability.

Table 1. Electronic properties of pristine twisted nanographenes.

Compound	DFT data [eV][a]			E_G^{opt}
	E_{HOMO}	E_{LUMO}	E_G	[eV][b]
N1	−5.54	−1.86	3.68	2.53
N2	−5.74	−1.62	4.11	2.99
N3	−5.67	−1.72	3.95	2.88
N7	−6.24	−0.92	5.32	4.07
N8	−6.20	−0.89	5.31	3.94
N9	−5.83	−1.38	4.46	3.26
N10	−5.89	−1.30	4.59	3.31
N11	−5.65	−1.69	3.96	2.92
N12	−5.63	−1.74	3.89	2.88
N13	−5.91	−1.27	4.64	3.40
N14	−5.68	−1.64	4.04	2.92
N15	−5.26	−2.25	3.01	2.43

[a] B3LYP/6-311G; values of the HOMO–LUMO gap (E_G) are given. [b] Optical gap, $E_G^{opt} = 1240/\lambda_{onset}$.

Conclusions

In summary, this study has explored the alumina-assisted C–F bond activation for the construction of pristine non-planar nanographenes. Our results show that the suggested strategy appears to be superior for the construction of complex multihelical and non-classical nanostructures. The feasibility of the approach is demonstrated by the synthesis of twelve unprecedented PAHs π-isoelectronic to HBC, seven of which were obtained for the first time. It is also shown that the fluoroarene precursor molecules strictly follow the "HF-assembly program" and alternative cyclization pathways can be rationalized from the precursor structure and thus can be controlled by the proper design of the precursor. Our approach provides facile access to elusive nanographenes, opening new opportunities to explore these unique materials.

Experimental Section

General procedure

Al_2O_3-Mediated HF Elimination. Typically, γ-Al_2O_3 (5–6 g) was initially dried at 250 °C for 30 min and then activated in a Schlenk line by annealing at 590 °C for 1 h under vacuum (10^{-2} mbar). After cooling to room temperature a flame-dried and nitrogen flushed microwave vial (2–5 mL) was charged with the respective fluorinated precursor (10 mg) and anhydrous *o*-DCB (4 mL). The activated γ-Al_2O_3 (2 g) was added to the mixture and the vial was sealed (nitrogen atmosphere). The condensation was carried out at 200–250 °C for the indicated time in the microwave. After completion of the reaction Al_2O_3 was extracted with hot toluene.

Acknowledgements

Funded by the Deutsche Forschungsgemeinschaft (DFG)—Projektnummer 182849149—SFB 953, AM407). The work was supported by Act 211 Government of the Russian Federation, contract N° 02.A03.21.0011. The authors are thankful to Dr. Frank Hampel for X-ray analysis of **P4** and **N11**. Open access funding enabled and organized by Projekt DEAL.

Conflict of interest

The authors declare no conflict of interest.

Keywords: aryl–aryl coupling · carbon origami · C–F bond activation · cyclodehydrofluorination · multihelical nanographenes

[1] Y. Segawa, H. Ito, K. Itami, *Nat. Rev. Mater.* **2016**, *1*, 15002.
[2] J. Wu, W. Pisula, K. Müllen, *Chem. Rev.* **2007**, *107*, 718–747.
[3] N. Savage, *Nature* **2011**, *479*, 557–559.
[4] K. P. Loh, S. W. Tong, J. Wu, *J. Am. Chem. Soc.* **2016**, *138*, 1095–1102.
[5] Y.-T. Wu, J. S. Siegel, *Chem. Rev.* **2006**, *106*, 4843–4867.
[6] Y.-T. Wu, J. S. Siegel, *Top. Curr. Chem.* **2014**, *349-355*, 63–120.
[7] P. W. Rabideau, A. Sygula, *Acc. Chem. Res.* **1996**, *29*, 235–242.
[8] P. Sarkar, P. Dechambenoit, F. Durola, H. Bock, *Asian J. Org. Chem.* **2012**, *1*, 366–376.
[9] A. Pradhan, P. Dechambenoit, H. Bock, F. Durola, *J. Org. Chem.* **2013**, *78*, 2266–2274.
[10] E. U. Mughal, B. Neumann, H. G. Stammler, D. Kuck, *Eur. J. Org. Chem.* **2014**, 7469–7480.
[11] J. Luo, X. Xu, R. Mao, Q. Miao, *J. Am. Chem. Soc.* **2012**, *134*, 13796–13803.
[12] K. Y. Cheung, X. Xu, Q. Miao, *J. Am. Chem. Soc.* **2015**, *137*, 3910–3914.
[13] K. Kato, Y. Segawa, L. T. Scott, K. Itami, *Chem. Asian J.* **2015**, *10*, 1635–1639.
[14] Y. Hu, X. Y. Wang, P. X. Peng, X. C. Wang, X. Y. Cao, X. Feng, K. Müllen, A. Narita, *Angew. Chem. Int. Ed.* **2017**, *56*, 3374–3378; *Angew. Chem.* **2017**, *129*, 3423–3427.
[15] T. Fujikawa, Y. Segawa, K. Itami, *J. Am. Chem. Soc.* **2015**, *137*, 7763–7768.
[16] Y. Li, Z. Jia, S. Xiao, H. Liu, Y. Li, *Nat. Commun.* **2016**, *7*, 11637.
[17] M. Grzybowski, K. Skonieczny, H. Butenschoen, D. T. Gryko, *Angew. Chem. Int. Ed.* **2013**, *52*, 9900–9930; *Angew. Chem.* **2013**, *125*, 10084–10115.
[18] P. Rempala, J. Kroulík, B. T. King, *J. Org. Chem.* **2006**, *71*, 5067–5081.
[19] L. Zhai, R. Shukla, S. H. Wadumethrige, R. Rathore, *J. Org. Chem.* **2010**, *75*, 4748–4760.
[20] M. Müller, H. Mauermann-Düll, M. Wagner, V. Enkelmann, K. Müllen, *Angew. Chem. Int. Ed. Engl.* **1995**, *34*, 1583–1586; *Angew. Chem.* **1995**, *107*, 1751–1754.
[21] X. Dou, X. Yang, G. J. Bodwell, M. Wagner, V. Enkelmann, K. Müllen, *Org. Lett.* **2007**, *9*, 2485–2488.
[22] V. S. Iyer, K. Yoshimura, V. Enkelmann, R. Epsch, J. P. Rabe, K. Müllen, *Angew. Chem. Int. Ed.* **1998**, *37*, 2696–2699; *Angew. Chem.* **1998**, *110*, 2843–2846.
[23] K. Y. Amsharov, M. A. Kabdulov, M. Jansen, *Chem. Eur. J.* **2010**, *16*, 5868–5871.

[24] K. Fuchibe, Y. Mayumi, N. Zhao, S. Watanabe, M. Yokota, J. Ichikawa, *Angew. Chem. Int. Ed.* **2013**, *52*, 7825 – 7828; *Angew. Chem.* **2013**, *125*, 7979 – 7982.
[25] N. Suzuki, T. Fujita, J. Ichikawa, *Org. Lett.* **2015**, *17*, 4984 – 4987.
[26] X. Tian, L. M. Roch, K. K. Baldridge, J. S. Siegel, *Eur. J. Org. Chem.* **2017**, 2801 – 2805.
[27] N. Suzuki, T. Fujita, K. Y. Amsharov, J. Ichikawa, *Chem. Commun.* **2016**, *52*, 12948 – 12951.
[28] K. Y. Amsharov, M. Kabdulov, M. Jansen, *Angew. Chem. Int. Ed.* **2013**, *52*, 7825—87825; *Angew. Chem.* **2012**, *124*, 4672 – 4675.
[29] K. Y. Amsharov, P. Merz, *J. Org. Chem.* **2012**, *77*, 5445 – 5448.
[30] O. Papaianina, V. A. Akhmetov, A. A. Goryunkov, F. Hampel, F. W. Heinemann, K. Y. Amsharov, *Angew. Chem. Int. Ed.* **2017**, *56*, 4834 – 4838; *Angew. Chem.* **2017**, *129*, 4912 – 4916.
[31] O. Papaianina, K. Y. Amsharov, *Chem. Commun.* **2016**, *52*, 1505 – 1508.
[32] A. K. Steiner, K. Y. Amsharov, *Angew. Chem. Int. Ed.* **2017**, *56*, 14732 – 14736; *Angew. Chem.* **2017**, *129*, 14926 – 14931.
[33] D. Sharapa, A. K. Steiner, K. Amsharov, *Phys. Status Solidi B* **2018**, *255*, 1800189.
[34] V. Akhmetov, M. Feofanov, S. Troyanov, K. Y. Amsharov, *Chem. Eur. J.* **2019**, *25*, 1910 – 1913.
[35] Y. Fujimaki, M. Takekawa, S. Fujisawa, S. Ohshima, Y. Sakamoto, *Polycyclic Aromat. Compd.* **2004**, *24*, 107 – 122.
[36] K. Matsui, M. Fushimi, Y. Segawa, K. Itami, *Org. Lett.* **2016**, *18*, 5352 – 5355.
[37] R. A. Pascal, W. D. McMillan, D. Van Engen, R. G. Eason, *J. Am. Chem. Soc.* **1987**, *109*, 4660 – 4665.
[38] L. Barnett, D. M. Ho, K. K. Baldridge, R. A. Pascal, *J. Am. Chem. Soc.* **1999**, *121*, 727 – 733.
[39] N. P. Hacker, J. F. McOmie, J. Meunier-Piret, M. Van Meerssche, *J. Chem. Soc. Perkin Trans. 1* **1982**, 19 – 23.
[40] D. Peña, D. Pérez, E. Guitián, L. Castedo, *Org. Lett.* **1999**, *1*, 1555 – 1557.
[41] R. W. Miller, S. E. Averill, S. J. Van Wyck, A. C. Whalley, *J. Org. Chem.* **2016**, *81*, 12001 – 12005.
[42] K. Y. Cheung, C. K. Chan, Z. Liu, Q. Miao, *Angew. Chem. Int. Ed.* **2017**, *56*, 9003 – 9007; *Angew. Chem.* **2017**, *129*, 9131 – 9135.
[43] C. Zhu, Y. Zhao, D. Wang, W.-Y. Sun, Z. Shi, *Sci. Rep.* **2016**, *6*, 33131.
[44] R. A. Pascal, W. D. McMillan, D. Van Engen, *J. Am. Chem. Soc.* **1986**, *108*, 5652 – 5653.
[45] M. Daigle, A. Picard-Lafond, E. Soligo, J. F. Morin, *Angew. Chem. Int. Ed.* **2016**, *55*, 2042 – 2047; *Angew. Chem.* **2016**, *128*, 2082 – 2087.
[46] A. Jančařík, J. Rybáček, K. Cocq, J. Vacek Chocholoušová, J. Vacek, R. Pohl, L. Bednárová, P. Fiedler, I. Císařová, I. G. Stará, *Angew. Chem. Int. Ed.* **2013**, *52*, 9970 – 9975; *Angew. Chem.* **2013**, *125*, 10154 – 10159.

Manuscript received: July 23, 2020
Accepted manuscript online: September 1, 2020
Version of record online: March 23, 2021

